Received: August 27, 2023. Revised: November 9, 2023.

International Journal of
Intelligent Engineering & Systems

http://www.inass.org/

Automated Inhomogeneity Correction and Fat Extraction in T1-weighted MRI of Long Bones: An Adaptive Disk Structure Element Morphological (ADSEM) Approach for Improved Osteosarcoma Diagnosis and Analysis

Mohamad Haizan Othman[1,2] Belinda Chong Chiew Meng[1]* Nor Salwa Damanhuri[1]
Mohd Ezane Aziz[2] Nor Azlan Othman[1]

[1]Biomedical Engineering and Intelligent System (BioMIS) Research Group, Centre for Electrical Engineering Studies, Universiti Teknologi MARA, Cawangan Pulau Pinang, 13500 Permatang Pauh, Pulau Pinang, Malaysia
[2]Department of Radiology, Universiti Sains Malaysia, Jalan Raja Perempuan Zainab II, Kubang Kerian, 16150 Kota Bharu, Kelantan
* Corresponding author's Email: belinda.chong@uitm.edu.my

Abstract: Fat extraction is a crucial aspect of diagnostic analysis in T1-weighted magnetic resonance imaging (MRI) images. However, the accuracy is affected by image inhomogeneity. Inhomogeneity refers to variations in signal intensity across an image, which can be caused by uneven magnetic fields or abnormal fluids in MRI image. This study uses fuzzy C-means (FCM) algorithm for fat region extraction. However, FCM is struggle with regions of similar intensity. The objective of this study is to propose a method for inhomogeneity correction using adaptive disk structure element morphological (ADSEM) approach. This rectifies the impact of inhomogeneity-induced intensity variations. The method is then integrated with FCM for fat extraction. This approach overcome FCM's intensity similarity limitation, enhancing fat extraction accuracy. Comparative assessments highlight the integrated ADSEM-FCM method's superiority over FCM. The quantitative assessment for proposed method in term of accuracy, recall, precision and F1 score is 0.9246, 0.9777, 0.7740, and 0.8526 respectively.

Keywords: Inhomogeneity correction, Fat extraction, Fuzzy C-means, Morphological, Structure element.

1. Introduction

Osteosarcoma is a rare and aggressive bone cancer that predominantly affects individuals during their rapid growth phases, especially in children, adolescents, and young adults [1]. Osteosarcoma exhibits a predilection for the lower body, with approximately 75% of cases occurring in the lower extremities, encompassing the pelvis (15%) and the distal femur and proximal tibia (60%). Conversely, the upper body constitutes about 18% of osteosarcoma occurrences, distributed as 8% in the jaw and 10% in the proximal humerus. The remaining 7% are scattered across other bones including the skull, ribs, lower arm, hand, spine, and sternum. Remarkably, the femur and tibia stand out as the most commonly affected bones [2].

Magnetic resonance imaging (MRI) serves as a pivotal diagnostic tool in osteosarcoma due to its exceptional proficiency in imaging musculoskeletal structures, including both soft tissue and bone [3]. MRI encompasses a diverse array of sequences. Specifically, longitudinal relaxation time (T1-weighted) provide essential information of anatomical view of the tissue which are fat, muscle and bone region. Moreover, MRI provides imaging across three distinct planes: axial, coronal, and sagittal [4], ensuring comprehensive visualization of osteosarcoma's anatomical context and aiding in precise diagnostic evaluations. T1-weighted imaging highlights anatomical structures, offering excellent tissue contrast and depicting fat as bright and fluid as dark [5, 6].

In clinical practice, radiologists rely on T1-weighted images to suppress fat signals, enabling

(a) (b) (c)

Figure. 1 Comparison between: (a) Normal, (b) Inhomogeneity due to uneven magnetic field, and (c) Inhomogeneity due to abnormal fluid

precise analysis of pathological features, such as those seen in osteosarcoma [7]. This manual method presents several challenges such as subjective, prone to variability, and time-consuming. Due to this, it highlighting the need for more efficient and objective techniques for accurate diagnosis and assessment [8, 9].

In addition, the accurate interpretation of these images is significantly challenged by intensity inhomogeneity, which refers to variations in signal intensity across an image. Inhomogeneity can result from various factors, including the inherent uneven magnetic field of MRI machines and the presence of abnormal fluids within the patient's body [10, 11].

Addressing inhomogeneity is crucial for accurate fat region extraction in T1-weighted MRI images. Alternatively, the field has explored automated solutions utilizing algorithms to correct inhomogeneity. Among these algorithms, the fuzzy C-means (FCM) algorithm is frequently employed for image segmentation [11].

However, FCM has its limitations. It can be sensitive to the initial selection of cluster centers, potentially leading to suboptimal results [11]. In the presence of inhomogeneity, FCM's performance is hindered by its tendency to cluster regions with similar intensity values, leading to inaccurate fat region segmentation [12, 13].

Fig. 1 shows the comparison between normal T1-weighted MRI images and inhomogeneity of T1-weighted MRI images that causes by uneven magnetic field and abnormal fluid.

Fig. 1 (a) shows T1-weighted MRI images with consistent magnetic fields, ensuring uniform signal intensities. This uniformity enables clear tissue boundary definition of fat. Contrastingly, Fig. 1 (b) displays T1-weighted MRI images affected by inhomogeneity caused by varying magnetic fields from the MRI machine. Fig. 1 (c) presents T1-weighted images marred by inhomogeneity due to abnormal fluid within the fat region. Inhomogeneity introduces signal intensity variations, blurring tissue boundaries and hindering precise tissue differentiation, notably fat.

In the present of inhomogeneity, FCM tends to cluster regions with similar intensity values, potentially leading to inaccurate segmentation, especially for tissues with closely matched signal intensities [12]. Also, fat, and adjacent muscle tissue can exhibit similar intensity values due to its influence. It is challenging for FCM in distinguishing these tissue types solely based on intensity values [13].

Morphological dilation is a fundamental image processing technique that involves expanding the boundaries of objects in a binary image [8]. It works by overlaying a structuring element (SE) on the image and expanding the regions where the SE intersects with foreground pixels. The size and shape of the SE dictate the extent of dilation. By default, the SE is often manually fixed to a certain value [14]. However, this approach can be time-consuming and may require trial and error to achieve optimal results, especially when dealing with inhomogeneity.

This study proposes an adaptive disk structure element morphological (ADSEM) method to correct inhomogeneity in T1-weighted MRI image. The corrected T1-weighted image is then integrated with conventional FCM algorithm, ADSEM-FCM method to extract the fat region in the image. The purpose of ADSEM-FCM method is to compensate the inhomogeneity and then improve the accuracy of fat extraction in T1-weighted MRI images. ADSEM is designed to automatically adjust the size of the structuring element (SE) based on the image's characteristics and the degree of inhomogeneity. By doing so, it eliminates the need for manual adjustments to enhance the efficiency and objectivity of the inhomogeneity correction process.

This paper is organized as follows; section 2. Literature review, section 3. Research methodology, section 4. Results and discussion, and section 5. Conclusion.

2. Literature review

Inhomogeneity in medical imaging, such as MRI, refers to the non-uniformity of signal intensity across an image, resulting from factors like uneven magnetic fields or variations in tissue properties [15]. Correcting inhomogeneity is pivotal as it greatly enhances the accuracy of image segmentation which is a fundamental process in medical image analysis [16]. In addressing inhomogeneity, two primary approaches exist: hardware-based and algorithmic correction. Hardware correction involves adjustments to the imaging equipment such as the magnet but can be impractical due to its high cost and complexity [17]. Conversely, algorithmic methods,

offer efficient, cost-effective solutions by adaptively compensating for inhomogeneity during image processing, thereby streamlining the segmentation process while maintaining precision and cost-effectiveness.

In the research conducted by Jianhua Song *et al*., [18], they addressing challenges in brain MR imaging, such as inhomogeneity and noise caused by suboptimal field uniformity and eddy currents. Conventional FCM clustering methods, relying on local spatial constraints, often yield unsatisfactory results. They introduce an approach that simultaneously corrects intensity inhomogeneity and improves segmentation using an objective function based on spatial coherence. Their method employs a unique similarity measure that considers local neighbouring information, enhancing MR data separability. Additionally, it incorporates an adaptive nonlocal spatial regularization term to overcome limitations of local spatial information, effectively handling noise and bias field estimation in the study.

V. Venkatesh *et al*., [19] introduces "InhomoNet," a network for MRI intensity inhomogeneity correction. It utilizes a multi-scale local information module and attention-driven skip connections for accurate feature capture. However, the method relies on supervised learning and necessitates ground truth data during training, which can be challenging to obtain accurate real-world scenarios with limited expert annotations. This dependency on ground truth data restricts its application to datasets with potential variability and uncertainty.

An automatic method present by Hui Liu *et al*., [20] for reducing inhomogeneity in liver MRI. The method utilizes global and local intensity information, as well as spatial continuity, while preserving grey levels for subsequent analysis. A constraint term ensures appropriate correction, and a fuzzy membership mask is used to remove noise. However, the method's sensitivity to initialization and parameters, along with its impact on other image features, it is necessitating further investigation.

Maryjo M. George *et al*. [21] introduce an effective correction which utilizes spatially constrained FCM clustering and anisotropic diffusion for compensation. However, the method's convergence time for real data may be a limitation, and further investigation is needed to assess its generalizability to diverse MRI datasets and impact on other image features. Comprehensive comparison with state-of-the-art methods is also necessary for a stronger assessment of its performance.

Mingming Chen *et. al*. [22] highlight a problem of inhomogeneity. To overcome the limitation, the study introduces an approach using a modified FCM algorithm. This innovative method outperforms existing approaches, underscoring its potential to enhance binarization accuracy, with implications extending to diverse applications in optical fringe pattern analysis. The limitation is the performance may be affected by complex pixel interactions in intricate patterns.

Sandhya Gudise *et. al.* discovered that the presence of inhomogeneity poses a significant challenge for brain segmentation [23]. The study proposed chaotic enhanced firefly algorithm integrated with fuzzy C-means (CEFAFCM) to improve the inhomogeneity. The method combines a spatially modified FCM with firefly algorithm and chaotic map for initialization. However, this method suffers a drawback of database-specific results that need broader dataset validation.

In conclusion, addressing inhomogeneity in medical imaging is crucial for accurate segmentation. Existing methods have limitations; for instance, some rely on ground truth data, while others suffer from sensitivity to initialization or convergence issues. Moreover, existing studies demonstrate that conventional FCM has limitations in handling local spatial information, which results in noise, such as inhomogeneity, significantly affecting the study's accuracy. In this study, we present an adaptive morphological method to compensate inhomogeneity. The method is then integrated with FCM for fat extraction. This integration method could improve fat region extraction, making it a valuable tool for enhancing the quality and reliability of fat region segmentation in clinical settings.

3. Proposed methodology

The proposed ADSEM-FCM method is a method that integrates ADSEM with conventional FCM to extract fat in T1-weighted MRI image. In ADSEM, the morphological operation consists of dilation and erosion operator that based on adaptive SE for image processing. FCM is used to cluster the MRI image into three clusters where the region with the highest intensity is the fat. Eq. (1) shows the equation for FCM algorithm to cluster the fat region.

$$J = \sum_{i=1}^{c} \sum_{j=1}^{N} \mu_{ij}^{m} \parallel x_j - c_i \parallel^2 \qquad (1)$$

Where:

' J ' represents the objective function that the FCM algorithm aims to minimize.

' c ' is the number of clusters.

'N' is the total number of data points.

' $\mu\ ij$ ' represents the membership value of data point

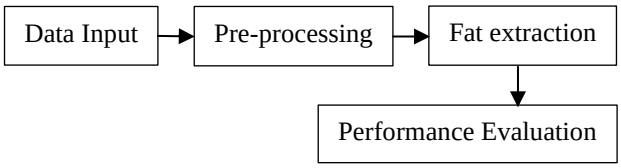

Figure. 2 Overall processes of proposed method

' j ' for cluster ' i.'
' m ' is a fuzzifier parameter, which is usually set to a value greater than 1. It controls the degree of fuzziness in the membership values.
'x_j' represents the data point ' J.'
'c_i' represents the center of cluster ' i.'
' $\| x_j - c_i \|$ ' represents the Euclidean distance between data point ' j ' and the center of cluster ' i.'

ADSEM is a method that used adaptive disk SE in the process of morphological to correct inhomogeneity in the MRI image. Fig. 2 shows the overall process of this study. Basically, it consists of four main processes which are data input, image pre-processing, fat extraction and performance evaluation.

3.1 Data input

The data collection was conducted at Hospital University Sains Malaysia (HUSM), Kubang Kerian, Kelantan, involving T1-weighted sequences of long bones (femur and tibia). There are 70 images collected which consists of 50 femur and 20 tibia MRI images. Ethical approval (reference number: USM/JEPeM/22060378) was obtained to ensure patients' rights and privacy protection. Informed consent was secured from patients, and data were handled with strict security and confidentiality measures. Anonymization of data was performed to remove identifying information.

3.2 Image pre-processing

In this study, image pre-processing is an inhomogeneity correction process. Due to inherent limitation of intensity inhomogeneity in the MRI images, the proposed ADSEM method is designed to correct inhomogeneity to improve the fat extraction process.

The flowchart in Fig. 3 depicts a step-by-step ADSEM method in the process of image pre-processing to correct inhomogeneity in T1-weighted MRI images. The process begins with the T1-weighted MRI image as input and converts it into a binary image using global thresholding. Eq. (1) is the global thresholding equation used to compute the threshold value.

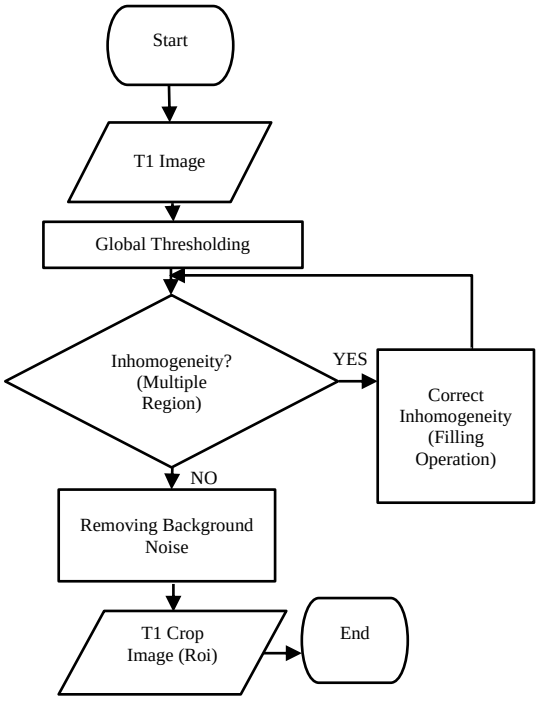

Figure. 3 The flowchart of ADSEM method

$$T = \frac{1}{2}(T_{max} + T_{min}) \quad (2)$$

Where:
T=Threshold value
T_{max}=maximum intensity value in the image
T_{min}=minimum intensity value in the image

This process initially separates the background (black region) and foreground which is object (white region) in T1-weighted MRI images. The edge of an object which is fat is connected if the image is clear without noise.

However, due to potential inhomogeneity arising, it will lead to a disconnected fat signal within the object. Therefore, multiple regions will be detected if there are disconnected fat signal. Preserving the continuity of the fat signal is crucial to ensure the entire object is accurately extracted, especially considering the entire object as the region of interested (ROI). This is because when the object is well-connected, the algorithm detects it as a single region; detecting multiple regions suggests inhomogeneity. To correct inhomogeneity, a filling operation is performed, and the resulting number of objects is counted. In cases where the ROI comprises only one object, inhomogeneity is absent. Detection of inhomogeneity triggers the "Correct Inhomogeneity" process, where the algorithm utilizing morphological dilation with an adaptive disk SE is applied. The SE size is dynamically adjusted through iterative dilation and fill hole operations, resolving inhomogeneity until a single-region image is achieved. Thus, the number of iterations is equal to

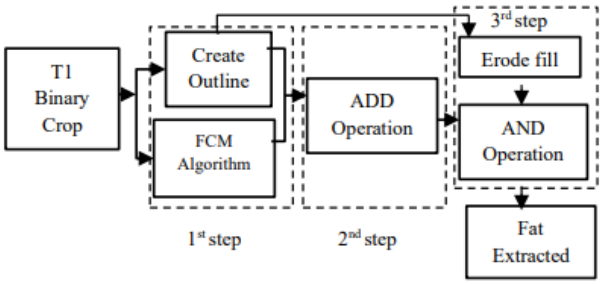

Figure. 4 Block diagram of ADSEM-FCM for fat extraction

the SE size. Conversely, if single region is achieved indicate the inhomogeneity is corrected then filling operation will be ended. Next, the background noise is removed by setting background pixel values to 0. Finally, a ROI is defined based on the single region in the image. The ROI is then cropped to focus on the informative area for further analysis.

3.3 Fat extraction

Fig. 4 shows the block diagram of ADSEM-FCM method for the process of fat extraction. This process integrated ADSEM and FCM for fat extraction. The process consists of three main steps. First step consists of "Create Outline" and "FCM Algorithm". Second step is integrating process using arithmetic ADD operation. Third step is morphological process and AND operation for fat extraction.

The first step involves two key stages: the "Create Outline" and the FCM algorithm. In the inhomogeneity correction process, the ROI obtained from the previous process is dilated. In the "Create Outline" process, the SE size from the ADSEM is employed for erosion, this will result in an erode fill image. The outline is then created through arithmetic subtraction of the dilated and eroded images.

Next process is FCM algorithm. The "FCM Algorithm" contributes by clustering the ROI into three distinct regions: high intensity (fat), intermediate intensity (muscle), and low intensity (cortical bone).

The FCM output pertaining to the fat region is integrated with the outline generated using morphological technique in previous create outline process to compensate the inhomogeneity. This process bridges gaps in inhomogeneity. The second step combined the output of "Create Outline" and "FCM Algorithm" by using ADD Operation. The third step, a logical AND operation is used to integrate with erode fill image from "Create Outline" process, this is to restore the mask to its original dimensions, thereby refining the accuracy of fat region extraction.

Table 1. The confusion matrix of four element

Actual Non-Fat	***Actual Fat***
Predicted Non-Fat (TN)	Predicted False Positive (FP)
Predicted False Negative (FN)	Predicted True Positive (TP)

3.4 Performance evaluation

The experiments were conducted using MATLAB 2019 on a laptop with an Intel Core i5 8th Gen processor and 8 GB of RAM. In this study, the proposed ADSEM-FCM method is experimented on 70 T1-weighted, axial MRI images. The experimental results were then compared against the ground truth. Table 1 shows the confusion matrix was constructed to assess the performance evaluation. It consists of four elements: True positive (TP), true negative (TN), false positive (FP), and false negative (FN).

Where:

i. True positive (TP): Represents the number of correctly identified fat regions, where the algorithm correctly classified pixels or regions as fat, and these were also accurately labelled as fat in the ground truth data.
ii. True negative (TN): Indicates the number of correctly identified non-fat regions, where the algorithm correctly classified pixels or regions as non-fat, and these were also accurately labelled as non-fat in the ground truth data.
iii. False positive (FP): Represents the cases where the algorithm incorrectly classified pixels or regions as fat when they were non-fat in the ground truth data.
iv. False negative (FN): Represents the instances where the algorithm incorrectly classified pixels or regions as non-fat when they were indeed fat in the ground truth data.

In this study, there are 4 major metrics are used as performance evaluation which are accuracy, precision, recall and F1 score.

i. Accuracy: The overall accuracy of the algorithm represents the proportion of correctly classified pixels to the total number of pixels in the image. Eq. (2) is the formula for accuracy.

$$Accuracy = \frac{TP+TN}{TP+FP+TN+FN} \quad (2)$$

ii. Precision: Precision measures the algorithm's ability to correctly identify fat regions among all the regions classified as fat. Eq. (3) shows the formula for precision.

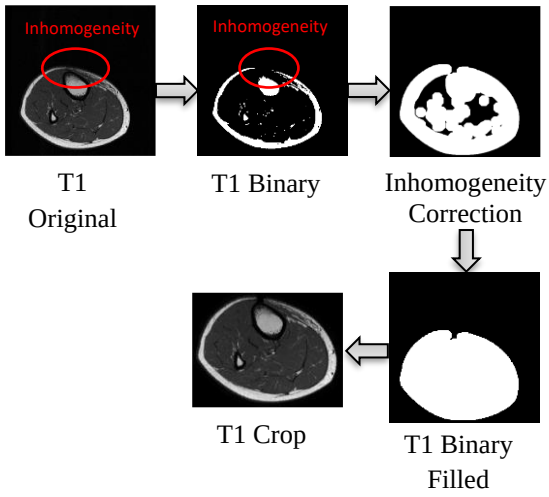

Figure. 5 The flow of proposed ADSEM method in intensity inhomogeneity correction

$$Precision = \frac{TP}{TP+TF} \quad (3)$$

iii. Recall: Also known as sensitivity, represents the algorithm's ability to correctly identify fat regions among all the actual fat regions present in the ground truth data. The formula as Eq. (4).

$$Recall = \frac{TP}{TP+FN} \quad (4)$$

iv. F1 Score: The F1 score is the harmonic mean of precision and recall, providing a balanced metric for both measures. The formula is shown by Eq. (5).

$$F1\ score = \frac{2xPrecisionxRecall}{Precision+Recall} \quad (5)$$

4. Results and discussions

4.1 Image pre-processing

Fig. 5 shows the flow of proposed ADSEM method in correcting the inhomogeneity. Due to the inhomogeneity, the fat region, which constitutes the outer region of the object, is disrupted, indicating a loss of fat information. When the fat is not covered the entire object, multiple regions is detected indicate that there is inhomogeneity in the image. In this situation, the filling process continues, during which the algorithm undergoes morphological dilation alongside an adaptive disk SE that autonomously adjusts its dimensions in response to the degree of inhomogeneity. The filling process is ended when there is a single region is detected where the binary filled mask is the resulting ROI mask. After that, the background noise is eliminated by assigning pixels to 0. This process eliminates irrelevant regions outside the object.

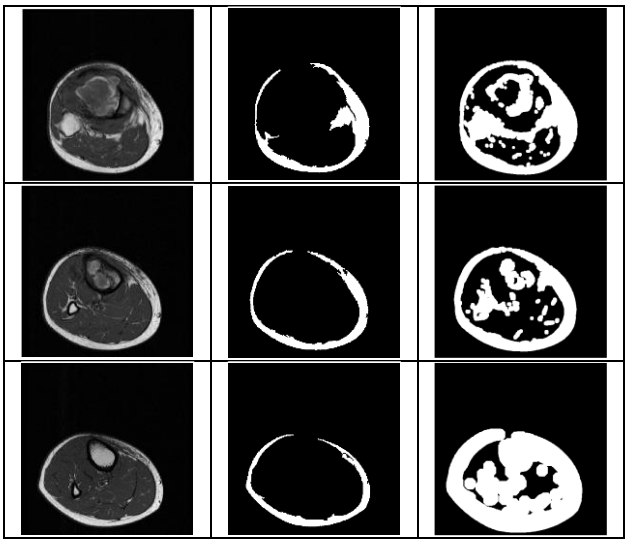

(a) (b) (c)

Figure. 6 Comparison between original T1-weighted image, image without inhomogeneity correction and inhomogeneity correction using ADSEM method: (a) Original T1-weighted, (b) Without inhomogeneity correction, and (c) With ADSEM inhomogeneity correction

Fig. 6 shows three visual comparisons of binary images obtained from T1-weighted MRI machine. The original T1-weighted MRI image is presented in the first column, serving as the baseline reference. The second column displays the binary image is created without inhomogeneity correction method.

As indicated, due to the presence of inhomogeneity, the outer region of the object is disconnected. Inhomogeneity can disrupt the continuity and clarity of features, leading to a less precise segmentation. In contrast, the third column showcases the binary image is created by using the ADSEM inhomogeneity correction method.

Therefore, it can be seen that the application of ADSEM effectively addresses the inhomogeneity issues present in the original image. The binary image created by using ADSEM method in the third column accurately outlines the ROI. The ADSEM method corrected the inhomogeneity and ensures the preservation of the important information within the fat regions. Hence, enhancing overall quality of ROI mask extraction and reliability of the fat extraction in the next segmentation process.

4.2 Fat extraction

The fat extraction process played a crucial role in delineating the fat regions within the T1-weighted MRI images. With the proposed ADSEM method the inhomogeneity is corrected. The output from ADSEM is then integrated with FCM to extract fat

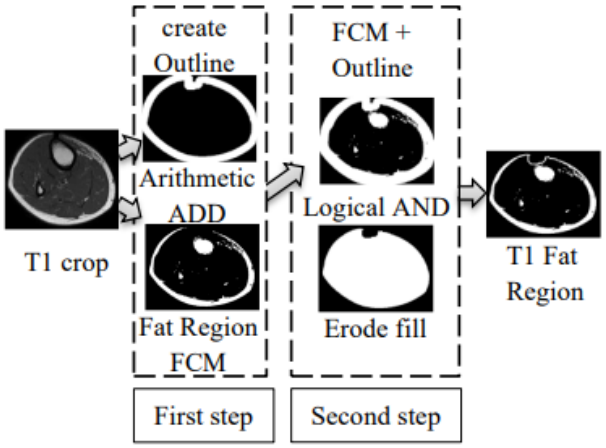

Figure. 7 Flow of fat extraction process

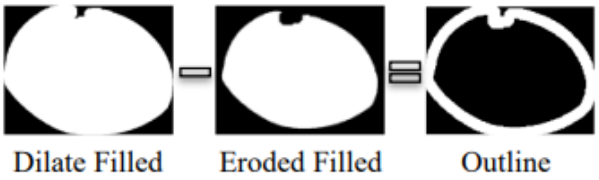

Figure. 8 Creating outline process

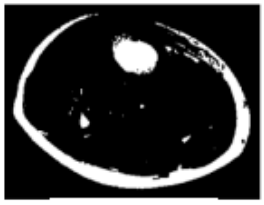

Figure. 9 Result from FCM process

region in the image. Fig. 7 shows the overall visual flow of fat extraction process after the inhomogeneity correction.

First step consists of "Create Outline" and FCM algorithm. Fig. 8 shows the process of creating outline where the dilated fill image from inhomogeneity correction process is used to form an outer layer of the ROI object. Using the SE size from the ADSEM dilate process to erode object the resultant ROI will be shrink to the size of original image. Subtracting the eroded filled image from dilated filled image, an outline is created.

Then FCM algorithm is applied to extract the fat region from ROI. Fig. 9 shows the fat region from FCM output. It can be observed that due to inhomogeneity, it's noticeable that the fat region, which forms the outer layer of the object, is disconnected.

To correct the inhomogeneity, the outline obtained from the process create outline is then integrated with FCM fat region using the arithmetic ADD operation. This process is important to make

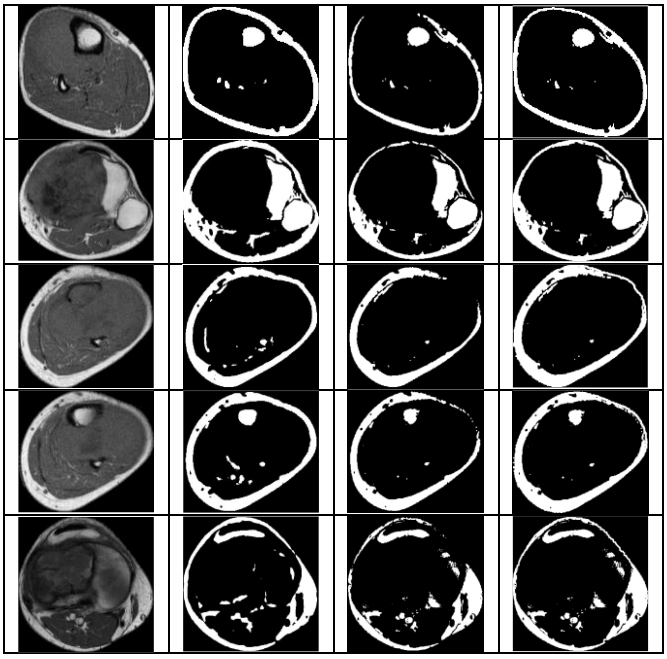

(a) (b) (c) (d)

Figure. 10 Output comparison of FCM algorithm and proposed ADSEM-FCM method: (a) T1 original images, (b) Ground truth, (c) FCM algorithm, and (d) Proposed ADSEM-FCM

Table 2. The average values of performance evaluation across all 70 slices of T1 MRI images between FCM and proposed ADSEM-FCM method

Method	**ACC**	**PREC**	**REC**	**F1**	**PT**
FCM	0.879	0.991	0.602	0.742	4.286
ADSEM-FCM	0.925	0.978	0.774	0.853	5.152

**In Table 2: ACC refer to ACCURACY, PREC refer to PRECISION, REC refer to RECALL, F1 refer to F1 Score, and PT refer to PROCESSING TIME.

sure the discontinuity of the region that cause by inhomogeneity is connected. Finally, logical AND operation is then applied between the resultant FCM outline image with erode fill image to restore the image into it original size.

4.3 Performance evaluation

Fig. 10 shows the comparison between original image, ground truth, FCM output and proposed ADSEM-FCM method output. In the figure, the original image consists of inhomogeneity. Due to inhomogeneity, FCM misses to segment some fat regions, resulting in loss of fat information. Conversely, the proposed ADSEM method correct inhomogeneity in T1-weighted image, the fat is covering the entire object, aligning with the ground truth. By integrating outline creation with the FCM algorithm, ADSEM-FCM method mitigates

inhomogeneity's impact on fat extraction. This improvement underscores its value for precise fat region assessment in T1-weighted MRI, particularly in inhomogeneous images.

Table 2 presented a concise summary of the performance evaluation for the integration of two methods employed in this study: FCM and ADSEM segmentation.

The performance evaluation can be observed that the ADSEM-FCM method outperforms the FCM method in several key aspects. ADSEM-FCM demonstrates higher accuracy (0.925 compared to 0.879), indicating its ability to achieve a higher proportion of correct classifications.

Precision refers to the ratio of true positive predictions to all positive predictions made by the algorithm. Often conventional FCM does not consider the spatial information in segmentation process. The influence of intensity inhomogeneity may falsely identify some pixel as fat. These false positive predictions lead to a higher precision value in FCM compared to ADSEM-FCM method which is 0.991 and 0.978 respectively.

Recall measures the algorithm's ability to capture all relevant instances, true positive pixels in the image. It measures the proportion of true positive predictions compared to all the pixels that are part of the true fat region in the image. In the comparison, it can be observed that ADSEM-FCM method has higher recall which is 0.774 compared to 0.602 for FCM. It shows that the ADSEM-FCM method helps in identifying the true fat regions more accurately, particularly in the presence of intensity inhomogeneity. As a result, the recall is higher for ADSEM-FCM because it accurately identifies more of the true fat region pixels, minimizing false negatives.

F1 Score, a harmonic mean of precision and recall, highlights the overall balance between precision and recall metrics. Even precision score is lower for ADSEM-FCM method, however it obtains a higher F1 Score of 0.853 compared to conventional FCM of 0.742. It indicates ADSEM-FCM method has better balance between precision and recall. Also, it shows that ADSEM-FCM method could minimize both false positives and false negatives when compared to conventional FCM.

In terms of processing time, ADSEM-FCM method does require slightly more time (5.152 seconds) than FCM (4.286 seconds). This is because ADSEM-FCM method employs an adaptive morphological technique to create outline that compensates for inhomogeneity. The extent of additional processing time depends on the severity of inhomogeneity, with need more processing especially for severe cases.

Overall, Table 2 underscores the advantages of the proposed ADSEM-FCM method over the conventional FCM approach, showcasing improved accuracy and effectiveness in fat region segmentation, even in the presence of intensity inhomogeneity. These results underscore the potential of ADSEM-FCM in enhancing medical image analysis, especially in applications such as osteosarcoma diagnosis and treatment.

5. Conclusion

This study proposed an adaptive morphological ADSEM method for inhomogeneity correction. ADSEM is then integrated with conventional FCM to create an outline for fat extraction. The proposed ADSEM-FCM algorithm effectively addresses the challenge of inhomogeneity, resulting in improved accuracy in fat region segmentation. The ADSEM-FCM method demonstrated superior performance compared to conventional FCM algorithm approaches, especially for images with varying degrees of inhomogeneity. The quantitative evaluation, based on accuracy, precision, recall, and F1 score, shows that the method's effectiveness in identifying fat regions. Further validation and exploration of the proposed method on diverse datasets and imaging modalities are recommended to enhance its generalizability and clinical impact.

Conflicts of interest

The authors declare no conflict of interest.

Author contributions

“Conceptualization, Mohamad Haizan Othman and Belinda Chong Chiew Meng; methodology, Mohamad Haizan Othman, Belinda Chong Chiew Meng and Mohd Ezane Aziz; software, Mohamad Haizan Othman, Belinda Chong Chiew Meng and Nor Azlan Othman; validation, Mohamad Haizan Othman, Belinda Chong Chiew Meng and Mohd Ezane Aziz; formal analysis, Mohamad Haizan Othman and Mohd Ezane Aziz; investigation, Mohamad Haizan Othman and Nor Salwa Damanhuri; resources, Mohd Ezane Aziz; data curation, Mohd Ezane Aziz; writing—original draft preparation, Mohamad Haizan Othman; writing—review and editing, Mohamad Haizan Othman and Belinda Chong Chiew Meng; visualization, Nor Salwa Damanhuri, Nor Azlan Othman and Mohd Ezane Aziz; supervision, Belinda Chong Chiew Meng, Nor Salwa Damanhuri and Mohd Ezane Aziz; project administration, Belinda Chong Chiew Meng;

funding acquisition, Belinda Chong Chiew Meng, Nor Salwa Damanhuri, Mohd Ezane Aziz and Nor Azlan Othman".

Acknowledgments

The authors express gratitude to the Ministry of Education Malaysia for the grant support under the Fundamental Research Funding (FRGS/1/2021/TK0/UITM/02/39) and to Universiti Teknologi MARA, Cawangan Pulau Pinang, and Hospital USM for generously providing research facilities for the successful conduct of this study.

References

[1] M. H. Othman, B. C. C. Meng, N. S. Damanhuri, M. E. Aziz, and N. A. Othman, "MRI Thigh Sequences in Determining the Tumor Size Using Fuzzy C-Means for Patients with Osteosarcoma", In: *Proc. of 2022 IEEE 12th International Conference on Control System, Computing and Engineering (ICCSCE*), pp. 125–130, 2022.

[2] M. Bernstein, H. Kovar, and M. Paulussen, "Ewing's Sarcoma Family of Tumors: Current Management", *Oncologist*, Vol. 11, No. 5, pp. 503–519, 2006, doi: 10.1634/theoncologist.11-5-503.

[3] A. L. Simon, A. Hallé, A. Tanase, M. Peuchmaur, P. Jehanno, and B. Ilharreborde, "Is magnetic resonance imaging reliable for assessing osteosarcoma of the knee joint in children?", *Orthop. Traumatol. Surg. Res.*, p. 103086, 2021.

[4] D. C. Alsop, E. Ercan, and O. Girard, "Inhomogeneous magnetization transfer imaging: Concepts and directions for further development", *NMR Biomed.*, Vol. 36, No. 6, p. e4808, 2023.

[5] Y. Shen, F. Gou, and Z. Dai, "Osteosarcoma MRI image-assisted segmentation system base on guided aggregated bilateral network", *Mathematics*, Vol. 10, No. 7, p. 1090, 2022.

[6] E. Kats, J. Goldberger, and H. Greenspan, "A soft STAPLE algorithm combined with anatomical knowledge", In: *Proc. of Medical Image Computing and Computer Assisted Intervention–MICCAI 2019: 22nd International Conference, Shenzhen, China, October 13–17, 2019, Proceedings, Part III 22*, pp. 510–517, Springer, 2019.

[7] K. Wang, A. Mamidipalli, and T. Retson, "Automated CT and MRI liver segmentation and biometry using a generalized convolutional neural network", *Radiol. Artif. Intell.*, Vol. 1, No. 2, p. 180022, 2019.

[8] S. Orgiu, C. L. Lafortuna, F. Rastelli, M. Cadioli, A. Falini, and G. Rizzo, "Automatic muscle and fat segmentation in the thigh from T1-Weighted MRI", *Journal of Magnetic Resonance Imaging*, Vol. 43, No. 3. pp. 601–610, 2016, doi: 10.1002/jmri.25031.

[9] B. C. C. Meng, U. K. Ngah, B. E. Khoo, I. L. Shuaib, and M. E. Aziz, "A framework of MRI fat suppressed imaging fusion system for femur abnormality analysis", *Procedia Computer Science*, pp. 808–817, 2015, doi: 10.1016/j.procs.2015.08.243.

[10] Y. Setiawan, C. Fatichah, and R. Sarno, "A new local gaussian variational level set for globus pallidus segmentation", *Int. J. Intell. Eng. Syst.*, Vol. 13, No. 5, pp. 317–326, 2020, doi: 10.22266/ijies2020.1031.29.

[11] P. Valsalan, P. Sriramakrishnan, and S. Sridhar, "Knowledge based fuzzy c-means method for rapid brain tissues segmentation of magnetic resonance imaging scans with CUDA enabled GPU machine", *J. Ambient Intell. Humaniz. Comput.*, pp. 1–14, 2020.

[12] G. A. Kumar and P. V Sridevi, "Brain tumor segmentation using chi-square fuzzy C-mean clustering", In: *Innovative Product Design and Intelligent Manufacturing Systems: Select Proceedings of ICIPDIMS 2019*, pp. 857–865, Springer, 2020.

[13] H. K. Lingappa, H. N. Suresh, and S. K. Manvi, "Medical image segmentation based on extreme learning machine algorithm in Kernel Fuzzy C-Means using artificial bee colony method", *Int. J. Intell. Eng. Syst.*, Vol. 11, No. 6, pp. 128–136, 2018, doi: 10.22266/IJIES2018.1231.13.

[14] N. Basty, Y. Liu, M. Cule, E. L. Thomas, J. D. Bell, and B. Whitcher, "Automated measurement of pancreatic fat and iron concentration using multi-echo and T1-weighted MRI data", In: *Proc. of 2020 IEEE 17th International Symposium on Biomedical Imaging (ISBI)*, pp. 345–348, 2020.

[15] U. Vovk, F. Pernus, and B. Likar, "A Review of Methods for Correction of Intensity Inhomogeneity in MRI", *IEEE Trans. Med. Imaging*, Vol. 26, No. 3, pp. 405–421, 2007, doi: 10.1109/TMI.2006.891486.

[16] S. Saman and S. J. Narayanan, "Active contour model driven by optimized energy functionals for MR brain tumor segmentation with intensity inhomogeneity correction", *Multimed. Tools Appl.*, Vol. 80, No. 14, pp. 21925–21954, 2021, doi: 10.1007/s11042-021-10738-x.

[17] E. N. Manson, S. Inkoom, and A. N. Mumuni,

"Impact of Magnetic Field Inhomogeneity on the Quality of Magnetic Resonance Images and Compensation Techniques: A Review", *Reports Med. Imaging*, Vol. 15, No. August, pp. 43–56, 2022, doi: 10.2147/RMI.S369491.

[18] J. Song and Z. Zhang, "Brain Tissue Segmentation and Bias Field Correction of MR Image Based on Spatially Coherent FCM with Nonlocal Constraints", *Comput. Math. Methods Med.*, Vol. 2019, p. 4762490, 2019, doi: 10.1155/2019/4762490.

[19] V. Venkatesh, N. Sharma, and M. Singh, "Intensity inhomogeneity correction of MRI images using InhomoNet", *Comput. Med. Imaging Graph.*, Vol. 84, 2020, doi: 10.1016/j.compmedimag.2020.101748.

[20] H. Liu, S. Liu, D. Guo, Y. Zheng, P. Tang, and G. Dan, "Original intensity preserved inhomogeneity correction and segmentation for liver magnetic resonance imaging", *Biomed. Signal Process. Control*, Vol. 47, pp. 231–239, 2019, doi: 10.1016/j.bspc.2018.08.005.

[21] M. M. George and S. Kalaivani, "A diffusion-based compensation approach for intensity inhomogeneity correction in MRI", *Int. J. Imaging Syst. Technol.*, Vol. 30, No. 3, pp. 761–778, 2020, doi: 10.1002/ima.22416.

[22] M. Chen, C. Tang, M. Xu, and Z. Lei, "Binarization of optical fringe patterns with intensity inhomogeneities based on modified FCM algorithm", *Opt. Lasers Eng.*, Vol. 123, pp. 14–19, 2019.

[23] S. Gudise, K. G. Babu, and T. S. Savithri, "An advanced fuzzy C-Means algorithm for the tissue segmentation from brain magnetic resonance images in the presence of noise and intensity inhomogeneity", *Imaging Sci. J.*, pp. 1–20, 2023.